



SAKARYA ÜNİVERSİTESİ

# FEN BİLİMLERİ ENSTİTÜSÜ DERGİSİ

Sakarya University Journal of Science  
SAUJS

e-ISSN 2147-835X | Period Bimonthly | Founded: 1997 | Publisher Sakarya University |  
<http://www.saujs.sakarya.edu.tr/en/>

Title: CFD Investigation of Different Flow Field Designs for Efficient PEMFC Performance

Authors: Safiye Nur ÖZDEMİR, İmdat TAYMAZ

Received: 2021-03-22 15:24:53

Accepted: 2021-04-11 15:07:09

Article Type: Research Article

Volume: 25

Issue: 3

Month: June

Year: 2021

Pages: 690-698

How to cite

Safiye Nur ÖZDEMİR, İmdat TAYMAZ; (2021), CFD Investigation of Different Flow Field Designs for Efficient PEMFC Performance. Sakarya University Journal of Science, 25(3), 690-698, DOI: <https://doi.org/10.16984/saufenbilder.901153>

Access link

<http://www.saujs.sakarya.edu.tr/en/pub/issue/62736/901153>

New submission to SAUJS

<http://dergipark.org.tr/en/journal/1115/submission/step/manuscript/new>

## CFD Investigation of Different Flow Field Designs for Efficient PEMFC Performance

Safiye Nur ÖZDEMİR<sup>1</sup>, İmdat TAYMAZ\*<sup>1</sup>,

### Abstract

Proton exchange membrane (PEM) fuel cell performance depends substantially on the geometry, configuration of the flow channels, and size. A right gas flow field pattern requires a homogeneous reactant distribution, low-pressure drop, and good water management. This paper outlines a numerical study, investigated the influence of the U-type, Z-type, and serpentine flow field configuration on the steady-state cell performance using the CFD technique ANSYS FLUENT PEMFC module. The main goal of this study focuses on a novel perspective for enhancing the design of the PEMFC resulting in better performance. The results indicate that the PEMFC with serpentine flow field configuration yields a significantly higher power density compared to the other designs.

**Keywords:** CFD, PEM Fuel Cell, Flow Field Design, Cell Performance, MPPT

### 1. INTRODUCTION

High efficiency, high power density, non-high operating temperatures, and environmental adaptability advantages significantly increase PEMFC's usability in the automotive industry compared to other fuel cells. Toyota Mirai, Honda Clarity, MAN Siemens, GM Opel, and Hyundai Nexo produce electric vehicles that run on fuel cell systems in the automotive industry, are a few of them [1]. However, some events such as reactant distributions, heat and mass transfer, and water flooding, which are directly related to the gas channel design, create problems in PEMFC [2]. Fuel cell flow field, is a main component of the fuel cell, which is of vital importance in the distribution of fuel gas and air, thermal

management, and removal of the water formed as a result of the electrochemical reaction from the fuel cell stack, shows diversity in the literature such as parallel, zigzag, pin type, serpentine and interdigitated design [3,4]. Figure 1 shows the schematic representation of the various flow patterns. There are lots of experimental and numerical studies on flow field design in the literature. Many studies focus on the improvement of reactant transport [5-7], cross-sectional geometry and dimensions of the channel [8,9], the number and geometry of the blockages located in the flow channel [10-12]. In recent years, there have been many studies based on flow field design. Yoon, Y.G. et al. examined four different rib widths of the flow field structures by keeping the channel width constant to get optimal

\*Corresponding author: taymaz@sakarya.edu.tr

<sup>1</sup>Sakarya University, Faculty of Engineering, Mechanical Engineering Department, Sakarya.

E-Mail: safiyeozdemir@sakarya.edu.tr

ORCID: <https://orcid.org/0000-0001-5025-5480>; <https://orcid.org/0000-0003-1337-7299>

cell performance based on experimental work. Increasing the flow field width results in higher current density regardless of full or less humidification. As a result of a conclusion drawn from this study, the best performance was achieved at a rib width is 0.5 mm, as narrow rib widths offer a wider gas flow area [13]. At first, a 3D PEMFC model based on a steady-state regime was developed, investigating the effect of the blockage rate of the baffle plate located in the center of the cathode gas channel on the cell performance. It was found that the power density obtained from baffle plate with a blockage ratio of 1 raised by 5.54 % percent compared to the straight flow field. In the second stage, the number of baffle plates is 1, 3, 5, and 7, respectively, and the effect of the baffle plate number on the power output has been examined in all cases the blockage rate keeping constant at 0.8. The peak performance was achieved when the number of the baffle plates was 5. The net power increase was measured as 9.39 % compared to the flow field without baffle plate [14]. Limjeerajarus and Charoen-amornkitt simulated 3-D, non-isothermal PEMFC models with six different flow field designs based on ANSYS FLUENT PEMFC module to evaluate the cell performance and transport phenomena. Optimal performance was obtained in the single serpentine flow area while the worst performance was obtained in the parallel flow area. However, the most important deflection of the single serpentine flow field design was that the power needed to meet for the pressure-drop is nearly ten times greater than the 3PIS (three-channel parallel in series) and 3S (three-channel serpentine) flow field designs and nearly twenty times greater than the 5PIS and 5S flow fields [15]. Shen et al. developed PEMFC with three different flow field structures (parallel, pressurized parallel, and single-serpentine) to explain that flow field design is a backbone that affects the fuel cell efficiency. Numerical simulations were carried out for three different flow fields at 338 K operating temperature and 1 atm operating pressure. The ratio of the Sherwood number, which expresses mass transfer, and the Euler number that describe the pressure drop, is a key factor in determining the fuel cell efficiency. In this study, the most suitable flow field design was

found using this factor. Although the cathode gas flow channel of the serpentine flow field design has a large pressure loss, better performance was achieved compared to the parallel flow field [16]. Shimpalee et al. tested the different number of gas flow channels on non-isothermal PEMFC with 200 cm<sup>2</sup> active area to investigate the reactant distribution and cell performance. Numerical simulations were realized using a commercial solver STAR-CD to specify and compare the current density distribution, membrane water content, and temperature distributions. It was recorded that the multi-channel PEMFC offers the most homogeneous current distribution [17]. Zhu and Zheng proposed a novel flow field configuration good at low-pressure drop, high power output, and much better water management compared to traditional gas flow field patterns. Rib width, channel depth, and channel width were analyzed numerically for the novel flow field design. It was discovered that the effect of the channel depth on cell performance compared to other parameters was not important. It was concluded that the radial gas flow field was more functional for maximum cell performance than parallel and serpentine flow field patterns [18].

Lots of studies based on flow field structure and optimization have been conducted in the literature. There are many numerical studies about the single-channel structure, but in reality, the PEMFC has many gas flow channels. There are few numerical publications available regarding different patterns in the bipolar plate with square geometry. In this study, a PEMFC model with different flow field designs was developed, and then the best flow field design that gives the highest cell performance using maximum power point tracking (MPPT) was determined and investigated.

## 2. MATERIALS AND METHODS

### 2.1. Model Description and Assumptions

In this study, numerical models of the PEMFC with 4.41 cm<sup>2</sup> active area for three different flow configurations were generated using a CAD software SolidWorks program. The numerical models consist of 10 number of flow channels in

both the cathode and anode. Figure 2 shows the flow directions of the fluid supplied to the cathode and anode channels of the PEMFC. The total length of the gas flow channels is 210 mm. The fluid and solid domains of the three different geometries were defined in ANSYS Design Modeler. Table 1 shows the geometric dimensions of the three different designs.

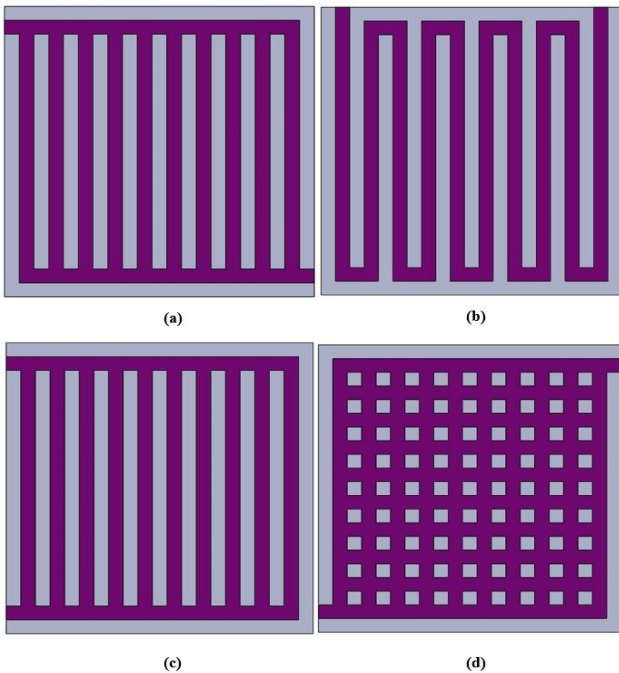


Figure 1 Schematic representation of different flow field designs (a) Z-type, (b) serpentine, (c) U-type, (d) pin-type

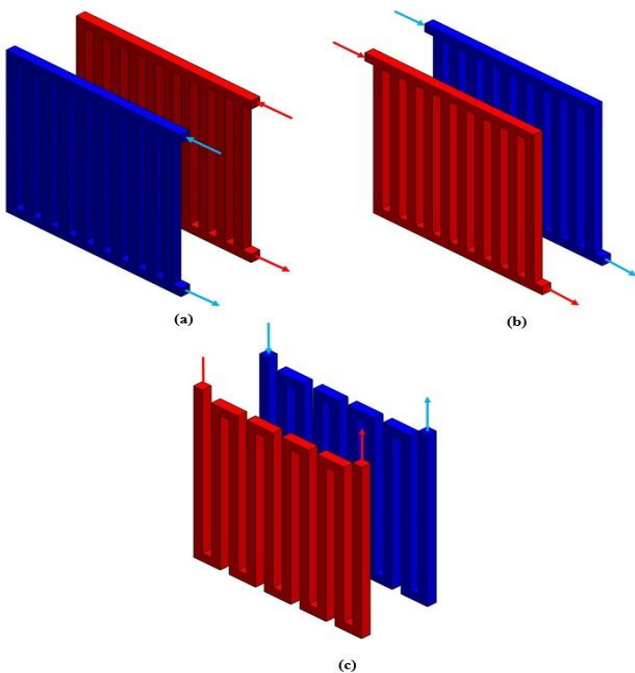


Figure 2 Flow directions in anode and cathode gas flow fields for (a) U-type (b) serpentine (c) Z-type

Table 1 Geometric dimensions

Parameters	Values	Units
Channel width	1	mm
Channel height	1	mm
Rib width	1	mm
Electrode width	21	mm
Electrode length	21	mm
Active area	4.41	cm <sup>2</sup>
Gas diffusion layer thickness	0.37	mm
Catalyst layer thickness	0.02	mm
Membrane thickness	0.178	mm

Mesh structures of the models were created in ANSYS Meshing 19.2. The most precise numerical solution is obtained from improved grid structure. The computation time is increased when the mesh is divided into very small elements. Therefore, mesh independence work has been carried out in numerical models. The most crucial requirement to obtain an accurate numerical solution in PEMFC is to construct the hexahedral mesh structure which is generated after mesh independence work. Three different geometries were discretized into 6 million cells and then, numerically solved. Figure 3 shows the grid structure of the numerical model with a serpentine flow field.

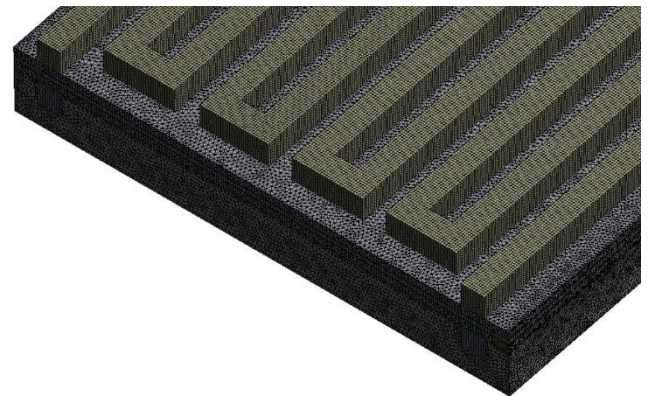


Figure 3 Mesh structure

Iteration independence study was carried out, and then, a convergent solution was obtained as a result of 500 iterations.

## 2.2. Boundary Conditions

After constructing the PEMFC geometry and mesh, boundary conditions should be defined for

each of the model domains. The input velocity of the hydrogen supplied to the anode channel, the input velocity of the air supplied to the cathode channel, and the mass fractions of the chemical species were calculated and defined in the FLUENT software. The hydrogen velocity entering the anode gas flow field is obtained as the following equation,

$$u_{a,in} = \zeta_a \frac{I}{2F} A_{MEA} \frac{1}{X_{H_2,in}} \frac{RT_{a,in}}{P_{a,in}} \frac{1}{A_{ch}} \quad (1)$$

The air velocity entering the cathode gas flow field is obtained as the following equation,

$$u_{c,in} = \zeta_c \frac{I}{4F} A_{MEA} \frac{1}{X_{O_2,in}} \frac{RT_{c,in}}{P_{c,in}} \frac{1}{A_{ch}} \quad (2)$$

where  $A_{MEA}$  is the active area of the membrane electrode assembly,  $I$  is the mean current density,  $\zeta$  is the stoichiometric flow rate and  $X$  is the molar fraction of hydrogen/oxygen. The outlet boundary condition of the anode and cathode flow fields typically was assigned as pressure. Since the outlet surfaces of the gas flow fields are exposed to the atmospheric pressure, they are assigned 1 atm. The operating pressure was selected as 303.975 kPa. The cathode terminal plate of the PEMFC is the surface on which current density values are obtained. The boundary conditions defined for the numerical solution are as in Table 2.

Table 2 Boundary conditions

Zone	Type	Unit	Value
<b>Anode Inlet</b>	Inlet velocity	m/s	Calculated
	Stoichiometry	-	2
	Temperature	K	343
	H <sub>2</sub> mass fraction	-	0.495
	H <sub>2</sub> O mass fraction	-	0.505
	Relative humidity	-	100%
<b>Cathode Inlet</b>	Inlet velocity	m/s	Calculated
	Stoichiometry	-	2
	Temperature	K	343
	O <sub>2</sub> mass fraction	-	0.217
	H <sub>2</sub> O mass fraction	-	0.0664
	Relative humidity	-	100%
<b>Outer Face</b>	Electric potential (anode)	V	0
	Electric potential (cathode)	V	Cell potential

<b>All Zones</b>	Operating pressure	kPa	303.975
------------------	--------------------	-----	---------

### 2.3. Solution Process

Numerical simulations were realized using ANSYS FLUENT 19.2 PEMFC add-on module to evaluate the performance. In order to find the answer to which gas flow channel design will result in the best performance, the same boundary conditions are defined for three different designs. For numerical solutions, three-dimensional, parallel processing, and double-precision were chosen. Biconjugate gradient stabilization (BCGSTAB) method and F-cycle were used for the solution of the consecutive governing equations system. Relaxation parameters were entered into the program as 0.95, 0.95, 0.7, and 0.3 for protonic potential, water content, pressure, and momentum, respectively to avoid the unstable numerical solution. Numerical simulations were performed on Intel(R) Core(TM) i7-7700HQ CPU (2.80 GHz, 16 GB RAM).

### 3. RESULTS AND DISCUSSION

In the present work, three different flow field configurations were analyzed numerically based on computational fluid dynamics (CFD) code. Overall assumptions and boundary conditions were the same to reveal the optimal flow area design. Reactants were fully humidified, CFD simulations were actualized at a constant temperature of 343 K. More precise results were obtained using a very small grid size. A numerical model was verified with experimental results of Wang et al. [19] with a straight flow field available in the literature. Figure 4 shows the numerical results are in good harmony with the experimental results. It has been observed that the current densities obtained at low cell potentials are higher than the experimental results. Water flooding, which significantly limits oxygen transport, will occur especially at high current densities, and since this situation is not taken into account in single-phase modeling, it is common to have inconsistencies at this point between the experimental results [20].

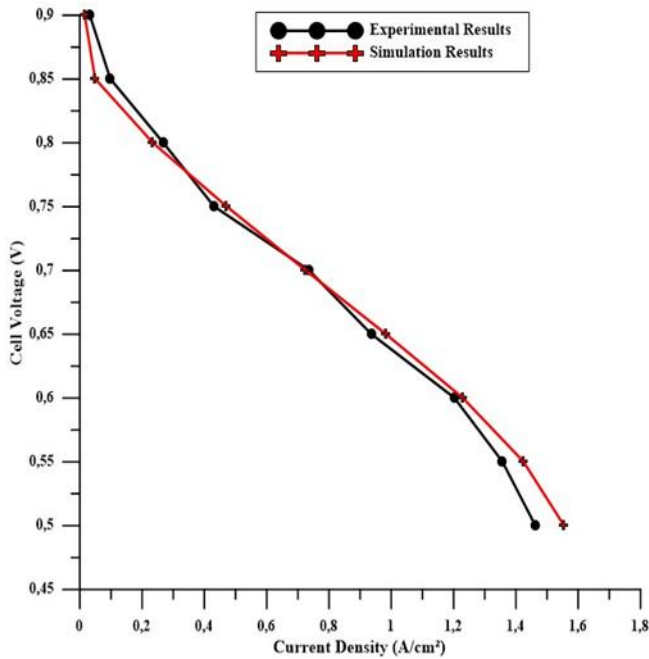


Figure 4 Experimental validation of the numerical results

Three different designs were compared on polarization and power curves. According to the polarization and power curves, the top performance was obtained from the serpentine flow field pattern, and the worst performance was obtained from the U-type flow field pattern. After the required boundary conditions of the PEMFC were defined, the program was run numerically for all three various flow field patterns. The open-circuit voltage is 1.1 V, starting from 0.45 V to be less than this value, the cell potentials have been assigned to the program with 0.05 increments up to 0.90 V. The current density values obtained for each cell potential defined on the cathode current collector plate wall were recorded. The current density-based cell potential (I-V) polarization curve and current density-based power density (I-P) power curve were shown in Figure 5. Numerical results show that the highest power density was obtained as  $7772 \text{ W/m}^2$  at 0.55 V cell voltage for serpentine flow field configuration. The maximum current densities are  $9964 \text{ A/m}^2$ ,  $13811 \text{ A/m}^2$  and  $16071 \text{ A/m}^2$  for the U-type, Z-type, and serpentine designs at 0.45 V operating voltage.

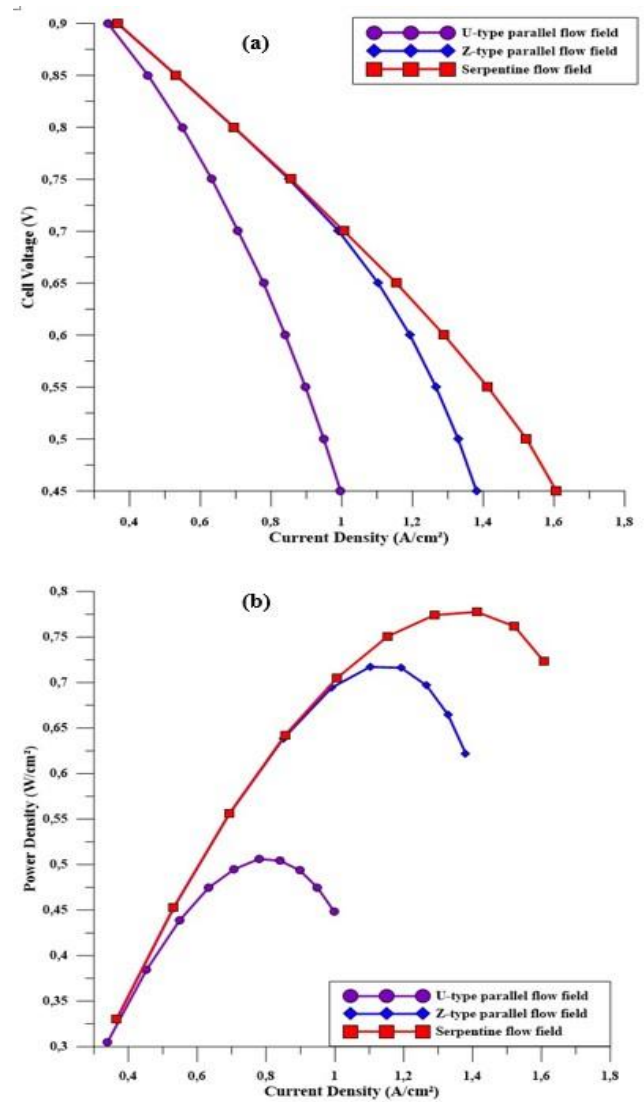


Figure 5 Polarization curve for (a) and power curve for (b) of the three different simulated arrangements ( $T=343 \text{ K}$ ,  $\varepsilon=0.8$ )

Figure 6 shows the oxygen concentration distribution at the interface of the GDL/CL (catalyst/gas diffusion layer) on the cathode side at operating voltage and operating temperature 0.65 V and 343 K, respectively. The oxygen mass fraction is high at the inlet of the cathode gas channel, decreasing gradually towards the channel outlet. The contours show that the most uniform oxygen distribution among the three designs is in the serpentine flow field. It results in the highest power income for the serpentine flow pattern compared to the other patterns. Maldistribution of the oxygen fraction negatively affected the performance of the U-type flow field. The reduction of the oxygen in the cathode gas

flow field is due to its consumption in the electrochemical reaction.

decreased from the PEMFC's inlet section to the outlet section because of the water accumulation.

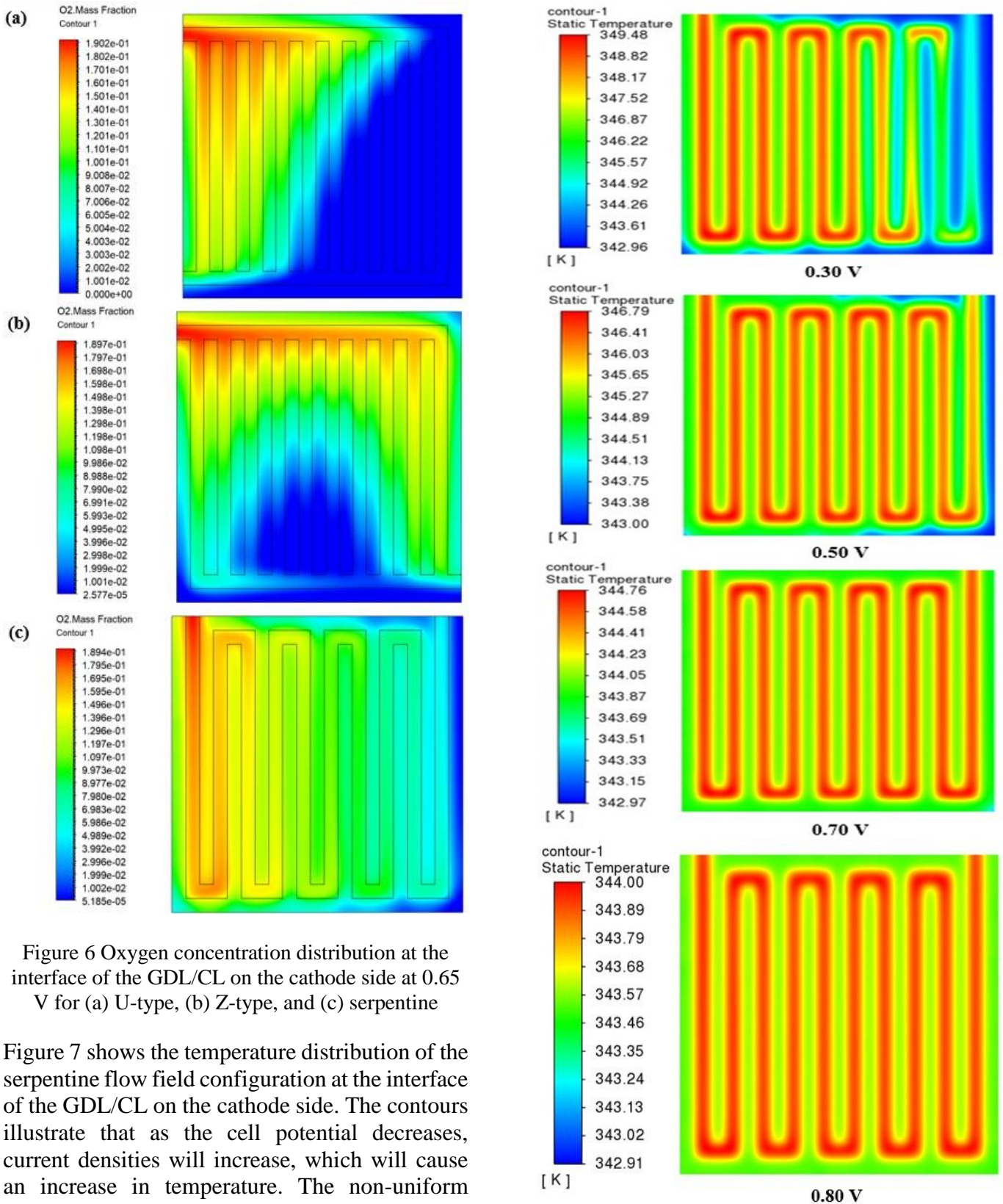


Figure 6 Oxygen concentration distribution at the interface of the GDL/CL on the cathode side at 0.65 V for (a) U-type, (b) Z-type, and (c) serpentine

Figure 7 shows the temperature distribution of the serpentine flow field configuration at the interface of the GDL/CL on the cathode side. The contours illustrate that as the cell potential decreases, current densities will increase, which will cause an increase in temperature. The non-uniform temperature distribution in the active area is observed more clearly at low cell potentials. It was discovered that the temperature gradually

Figure 7 Temperature distribution for various operating voltages

It is concluded that the maximum temperature differences are 6.52 K, 3.79 K, 1.79 K, and 1.09 K at 0.30 V, 0.50 V, 0.70 V, and 0.80 V cell voltages, respectively. Figure 8 shows the water concentration distribution at the interface of the GDL/CL layer on the cathode side at operating voltage and operating temperature 0.65 V and 343 K, respectively. The water mass fraction increased towards the cathode gas flow field outlet section because of the oxygen reduction reaction. A certain level of humidification is essential for the fuel cell to operate at optimum performance. Water accumulation will adversely affect the power output if not kept at a certain level. The water produced from the channel inlet to the outlet section has increased. The most important criterion to be considered in the PEMFC gas flow field is the pressure drop. Pressure loss in the gas flow channel can be compensated by the use of a compressor. The pressure loss, which tends to decrease towards the gas flow channel outlet, is the highest in the inlet section of the gas channel. The difference between the outlet and inlet sections of the cathode gas channel gives the pressure drop. Average flow velocity is increased with increasing pressure drop. Peak levels of pressure drop in U-type, Z-type, and serpentine flow fields are 25.81 kPa, 0.060 kPa, and 0.405 kPa, respectively. The main cause of pressure loss in gas flow channels is friction, however, it is caused

by the places where the flow maneuvers.

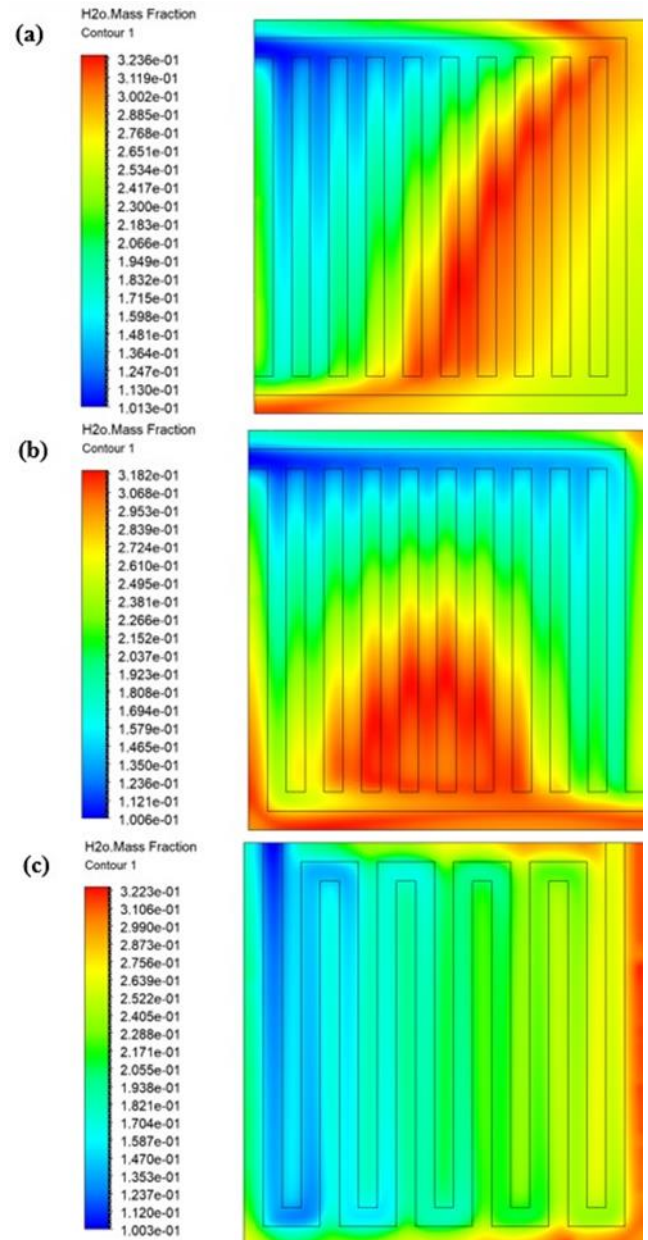


Figure 8 Water concentration distribution at the interface of the GDL/CL on the cathode side at 0.65 V for (a) U-type, (b) Z-type, and (c) serpentine

#### 4. CONCLUSION

A full three-dimensional PEMFC with an active area of 4.41 cm<sup>2</sup> (2.1 cm × 2.1 cm) was generated. Numerical work was carried out to investigate the impact of U-type, Z-type, and serpentine flow field configurations on cell performance. Model validation was performed for a PEMFC with a single straight flow field, and it was found that the simulation results and experimental data were matched with each other. When the cell potential is 0.70 V or above, the gas

flow field design is Z-type or serpentine, as can be seen from the polarization and power curves, it is observed that it creates any change in its effect on cell performance. When the cell potential was less than 0.70 V, Z-type and serpentine flow field designs substantially affected the cell performance. On the other hand, the worst cell performance was obtained in the U-type flow field pattern. In this study, the model that gives the superior cell performance among three different numerical models developed numerically was determined. This work can guide fuel cell stack manufacturers in terms of optimum flow field configuration. Design, operating parameters can be examined in detail for the best geometry in future work.

### ***Funding***

The authors have not received any financial support for the research, authorship or publication of this study.

### ***The Declaration of Conflict of Interest/ Common Interest***

No conflict of interest or common interest has been declared by the authors.

### ***Authors' Contribution***

The authors contributed equally to the study.

### ***The Declaration of Ethics Committee Approval***

This study does not require ethics committee permission or any special permission.

### ***The Declaration of Research and Publication Ethics***

The authors of the paper declare that they comply with the scientific, ethical and quotation rules of SAUJS in all processes of the paper and that they do not make any falsification on the data collected. In addition, they declare that Sakarya University Journal of Science and its editorial board have no responsibility for any ethical violations that may be encountered, and that this study has not been evaluated in any academic publication environment other than Sakarya University Journal of Science.

## **REFERENCES**

- [1] Wang, Y. et al. (2020) ‘Fundamentals, materials, and machine learning of polymer electrolyte membrane fuel cell technology’, Energy and AI. Elsevier Ltd, 1, p. 100014.
- [2] Pei, P. et al. (2016) ‘A review on water fault diagnosis of PEMFC associated with the pressure drop Fourier transform’, Applied Energy. Elsevier Ltd, 173, pp. 366–385.
- [3] Wilberforce et al. (2019) ‘A comprehensive study of the effect of bipolar plate (BP) geometry design on the performance of proton exchange membrane (PEM) fuel cells’, Renewable and Sustainable Energy Reviews. Elsevier Ltd, 111(April), pp. 236–260.
- [4] Kahraman, H. and Orhan, M. F. (2017) ‘Flow field bipolar plates in a proton exchange membrane fuel cell: Analysis & modeling’, Energy Conversion and Management. Elsevier Ltd, 133, pp. 363–384.
- [5] Perng, S. W. and Wu, H. W. (2015) ‘A three-dimensional numerical investigation of trapezoid baffles effect on non-isothermal reactant transport and cell net power in a PEMFC’, Applied Energy. Elsevier Ltd, 143, pp.81–95.
- [6] Liu, C. et al. (2006) ‘Reactant gas transport and cell performance of proton exchange membrane fuel cells with tapered flow field design’, Journal of Power Sources 158, pp. 78–87.
- [7] Yan, W. M. et al. (2008) ‘Effects of serpentine flow field with outlet channel contraction on cell performance of proton exchange membrane fuel cells’, Journal of Power Sources, 178(1), pp. 174–180.
- [8] Obayopo, S. O., Bello-Ochende, T. and Meyer (2011) ‘Performance enhancement of a PEM fuel cell through reactant gas channel and gas diffusion layer optimisation’, Africa, (November).

- [9] Ahmed, D. H. and Sung, H. J. (2006) 'Effects of channel geometrical configuration and shoulder width on PEMFC performance at high current density', *Journal of Power Sources*, 162(1), pp. 327–339.
- [10] Ozdemir and Taymaz (2021) 'Numerical investigation of the effect of blocked gas flow field on PEM fuel cell performance', *International Journal of Environmental Science and Technology*. Springer Berlin Heidelberg.
- [11] Shen et al. (2018) 'Performance investigation of PEMFC with rectangle blockages in Gas Channel based on field synergy principle', *Heat and Mass Transfer/Waerme- und Stoffuebertragung. Heat and Mass Transfer*.
- [12] Kuo, J. K., Yen, T. S. and Chen, C. K. (2008) 'Improvement of performance of gas flow channel in PEM fuel cells', *Energy Conversion and Management*, 49(10), pp. 2776–2787.
- [13] Yoon, Y. G. et al. (2004) 'Effects of channel configurations of flow field plates on the performance of a PEMFC', *Electrochimica Acta*, 50(2–3 SPEC. ISS.), pp. 709–712.
- [14] Yin, Y. et al. (2018) 'Numerical investigation on the characteristics of mass transport and performance of PEMFC with baffle plates installed in the flow channel', *International Journal of Hydrogen Energy*. Elsevier Ltd, 43(16), pp. 8048–8062.
- [15] Limjeerajarus, N. and Charoen-amornkitt, P. (2015) 'Effect of different flow field designs and number of channels on performance of a small PEFC', *International Journal of Hydrogen Energy*. Elsevier Ltd, 40(22), pp. 7144–7158.
- [16] Shen, J., Tu, Z. and Chan, S. H. (2020) 'Evaluation criterion of different flow field patterns in a proton exchange membrane fuel cell', *Energy Conversion and Management*. Elsevier, 213(April), p. 112841.
- [17] Shimpalee, S., Greenway, S. and Zee, J. W. Van (2006) 'The impact of channel path length on PEMFC flow-field design', 160(January), pp. 398–406.
- [18] Zhu, W. and Zheng, M. (2019) 'Radial flow field of circular bipolar plate for proton exchange membrane fuel cells', *International Journal of Heat and Technology*, 37(3), pp. 733–740.
- [19] Wang, L. et al. (2003) 'A parametric study of PEM fuel cell performances', *International Journal of Hydrogen Energy*, 28(11), pp. 1263–1272.
- [20] Nguyen, P. T., Berning, T. and Djilali, N. (2004) 'Computational model of a PEM fuel cell with serpentine gas flow channels', 130, pp.149–157.